Integration of Production Data with Numerical Sensitivity Coefficients: A Synthetic Example

Linan Zhang, Luciane Cunha, and Clayton V. Deutsch

Centre for Computational Geostatistics
Department of Civil and Environmental Engineering
University of Alberta

This paper presents the application of the methodology proposed in CCG Report Six (208) to a synthetic example. The historical data is from flow simulation with 2-D reference porosity and and permeability models. Initial porosity model and permeability models are created by SGS conditioning to well data. The initial models are then updated to match historical production data. The proposed methodology achieves a reasonable pressure and rate match. The methodology is checked and insight into inversion problems is gained.

Introduction

The fast approximation of sensitivity coefficients from two flow simulation runs was the essence of Zhang's Master's thesis. A real reservoir case study was shown in the thesis and in previous CCG reports; however, this paper presents an application to a synthetic example. Synthetic ex examples remove confounding factors such as relative permeability curves, permit fast application and consideration of multiple realizations and permit comparison to a reference.

This paper presents the generation of the true models and historical data, the creation of five initial realizations, application of the methodology to the realizations, results of sensitivity study, and comparison of the simulation results and linear approximation of the reservoir behavior.

The domain is 4000m × 4000m × 10m. The top surface changes from a depth 2700m on the western edge to 3100m on the eastern edge, shown in Figure 1. The 2-D grid system has 10,000 grid cells 100 40 m cells in X and Y direction. Sequential Gaussian Simulation (SGS) was used to generate the conditional realizations of permeability and porosity based the sample data shown below. The permeability mean is 387mD and porosity mean is 0.162.

Sample	Location in the X direction(m)	Location in the Y direction(m)	Porosity (fraction)	Permeability (mD)
1	420	820	0.1225	305
2	420	1820	0.2217	560
3	420	2820	0.1202	300
4	1820	1220	0.1268	250
5	1820	2220	0.2310	580
6	1820	3220	0.1682	360
7	3900	1020	0.2036	500
8	3900	2020	0.2036	500
9	3900	3020	0.2036	500

In order to increase heterogeneity of the models, the porosity and permeability realizations generated above were post-processed by setting the porosity and permeability as zeros at the grid blocks with permeability equal to or lower than 235mD (about 15% of the number of grid blocks) and setting the permeability as 750+(permeability -750)*3 at the grid blocks with permeability larger than 750mD. The images and histograms of the post-processed models are shown in Figures 2 and 3, respectively. These post-processed realizations are taken as the true reference models. The means of permeability and porosity for the post-processed models are 368mD and 0.144, respectively.

The well locations are shown in Figure 2 as white points. The wells with "Pro" in the names are producers and those with "Inj" are injectors. The permeability and porosity at wells:

Well Name	Location in the X direction(m)	Location in the Y direction(m)	Porosity (fraction)	Permeability (mD)
Pro 1	420	620	0.1289	333
Pro 2	420	1620	0.2060	1270
Pro 3	420	2620	0.1415	382
Pro 4	1820	820	0.1610	644
Pro 5	1820	2220	0.2310	580
Pro 6	1820	3620	0.1267	254
Inj 1	3900	1020	0.2036	500
Inj 2	3900	2020	0.2036	500
Inj 3	3900	3020	0.2036	500

The liquid production rate at producers and the injection rate at injectors were set as the input parameters for flow simulation:

Time Period / Well Name	273-3287 days	After 3288 days
Pro 1	50	130
Pro 2	50	250
Pro 3	50	170
Pro 4	210	0
Pro 5	360	0
Pro 6	235	0
Inj 1	325	165
Inj 2	335	235
Inj 3	330	195

The reference models shown in Figure 2 and homogeneous models with the constant permeability of 368mD and porosity of 0.144, were flow simulated. The results of flow simulation are shown in Figures 4 to 8. The reservoir/well behaviours between the heterogeneous models and homogeneous models are very different except Pro5's water cut and oil production rate. The oil production rate at the six

producers and well bottom-hole pressure at the six producers and three injectors from flow simulation for the reference models are used as historical data later in the application of the proposed methodology.

Five Initial Realizations and Flow Simulation Results

Five conditional permeability realizations were generated by SGS with anisotropy ranges of 1500m in the Y direction and 2500m in the X direction, spherical variogram, and the well data shown in Table 3. The images and histograms for the five conditional permeability realizations are shown in Figures 9 and 10. From Figures 9 and 10, it can be seen that the images and means of the five realizations are different from the reference model. The mean of permeability for the five realizations is higher than the reference permeability. This is because the wells are usually arranged in the high permeability regions. The results of production rate, water cut and well bottom hole pressure from flow simulation for the five realizations and reference models are shown in Figures 11 to 14. They are very different.

Conditioning to Flow Data

ECLIPSE was used for flow simulation. There are 10,000 grid blocks in the 2-D property models. The liquid production rate and water injection rate were input parameters. The well bottom hole pressure and the quarterly averaged oil production rate were the parameters to match. The permeability models were updated. The porosity model was co-simulated with permeability realization with a correlation coefficient of 0.7. The horizontal permeability values in the X and Y directions were set to be the same. One perturbation location per iteration was selected.

Twenty iterations were completed for updating each model. The perturbation locations are shown in Figure 15. Well locations are shown as circles. The perturbation locations are shown as solid circles named by "S" plus iteration number. The perturbation location for the twentieth iteration was set at one of the perturbation locations near the well with the highest mismatch after nineteen iterations.

The weights for pressure and fractional flow rate were kept the same at $w_p = w_q = 1$. Weights for the observed rates at each well, $\lambda_{w,q,t}$, were also kept the same. Weights for well bottom-hole pressure data, $\lambda_{w,p,t}$, are also set as the same. The data for all wells are equally weighted, β_w for every well. The perturbations were propagated by a Gaussian type of variogram with anisotropy ranges of 500m in the Y direction and 800m in the X direction.

The flow simulation results for reference models before 6025 days were used as historical data in the application. The reason for selecting such a long time is to assure a production period after water breakthrough for wells Pro1, Pro2 and Pro3.

The methodology was used to update the five realizations. The results of mismatch versus iteration are shown in Figure 16. The mismatch in pressure and production rate as well as global mismatch against the relevant base models is shown below. It can be seen that the methodology can reduce pressure mismatch and production rate mismatch for all five realizations. The mismatch in the fractional flow rate decreased by an average value of 74.6% for the five realizations. The pressure mismatch decreased by an average value of 68.1%.

Realization	Pressure mismatch (%)	Rate mismatch (%)	Global mismatch (%)
1	76.32	64.07	70.19
2	69.31	84.62	76.96
3	68.74	62.19	65.47
4	67.29	85.44	76.37
5	58.71	76.65	67.68

Comparison of the global mismatch for the five realizations against the mismatch value for the original realization #1 is shown in Figure 17. The global mismatch changes similarly for multiple realizations when the same set of perturbation locations is selected.

The comparison of field oil production rate between the original and updated realizations is shown in Figure 18. The history match period is before 6025 days. The reservoir behaviour after 6025 days is forecasted. Figure 18 shows that the reservoir behaviour for the updated realizations are much closer to historical data than those for the original realizations in the history match period and better except for realization #1 with no difference for the forecast period.

The comparison of oil production rate, field water cut and well bottom hole pressure for the original realization #2 and the updated realization #2 are shown in Figures 19 to 21. The history match period is before 6025 days. The well behaviours after 6025 days are forecasted. It can be seen that the well bottom hole pressure at all wells for the updated model are closer to historical data and the well production rates at some wells are improved.

Therefore, the simulation results for the updated models are much better than the original models for history match period and better for forecast period. The models post-processed by the proposed methodology are better for prediction.

Changes of Property Models

The comparison of images of the five updated realizations and reference model are shown in Figure 22. It can be seen that the methodology updated the realizations significantly to make them closer to the reference model. The updated realizations are similar. It should be noticed that well Pro5 for all the five realizations is in a low permeability region but is in a high permeability region for the reference model. This is because that there is a impermeable region between Pro5 and injectors in the reference model but no impermeable region was created in the five conditional realizations due to few perturbation locations between producers and injectors. Increasing one or two perturbation locations will improve the updated models.

Permeability difference between the true and the conditional realizations as well as their relevant histograms are shown in Figures 23 and 24. They show that the methodology can reduce the permeability difference and make the means of the difference between true and the updated realizations closer to zero.

Sensitivity Study

The sensitivity study here focuses on the effects of type of perturbation propagation, perturbation locations and range. The sensitivity study on the effect of propagation type on mismatch was conducted with realization #2. The perturbation locations were selected at 16 locations shown in Figure 25. Spherical type and Gaussian type of propagation were selected with the range of 500 meters. Two iterations were selected with the perturbation locations F and H. The results are shown in Figure 26. The mismatch of the updated model with Gaussian types of perturbation

propagation reaches lower levels, which means that the Gaussian type of propagation is better in this case.

A sensitivity study on effect of the order of perturbation locations was conducted with realization #2, range of 500m and the propagation of Gaussian type. The perturbation locations were selected at 16 locations shown in Figure 25. Two different ways were used in the application: one is to perturb the locations near wells at first, and the other is to perturb the locations far away from the wells at first. Seven perturbation locations far away from the wells and nine locations near the wells were selected for both of the two ways. The rule of selecting the perturbation locations near the wells is to select the location nearest to the well with the highest mismatch so that some locations were selected twice while some other locations were not selected. The rule of selecting the perturbation locations far away from wells is to select the location from the south to the north and from the east to west.

Figure 27 shows the mismatch change for the different orders of selected perturbation locations. Figure 27(a) corresponds to the case that the perturbations far from well locations were selected at first; Figure 27(b) corresponds to the case that the perturbations near well locations were selected at first. The mismatch results in Figure 27(b) are better because of the lower levels of pressure mismatch and rate mismatch as well as global mismatch.

A sensitivity study on effect of the range of perturbation propagation was conducted with realization #2, first selection of the locations near wells and the propagation of Gaussian type for perturbation. The perturbation locations were selected at 16 locations shown in Figure 27(b).

Figure 28 shows the mismatch change for the different ranges of propagation. Figure 28(a) corresponds to the case that the range of 400m; Figure 28(b) corresponds to the case that the range of 500m, which is half the well spacing in the rows from the south to the north. The results show that half the well spacing is a better option for the range of perturbation propagation.

A sensitivity study on effect of the porosity model was conducted with the conditional realization #1, selection of the locations near wells at first and the propagation of Gaussian type. In the methodology, there are two flow simulations at each iteration. One perturbation location is selected to perturb the permeability, then the first flow simulation runs with the perturbed permeability and porosity from the previous iteration. Then, the sensitivities with respect to the permeability change were calculated, which are used to get the optimal changes to update the permeability. After that, the porosity model is obtained by two different ways: (1) keeping the same model as the previous iteration, and (2) doing co-simulation with the updated permeability. The second flow simulation runs with the updated porosity and the updated permeability to check the well/reservoir behaviours.

Three cases were studied here. Firstly, the permeability realization #1 was updated by the methodology when the true porosity was used with the range of perturbation propagation of 500m. The perturbation locations are the perturbation locations for Figure 27(b) plus four locations successively selected near the well with the highest mismatch. The mismatch results are shown in Figure 29(a). This is Case 1. Secondly, the permeability realization #1 was updated by the methodology with co-simulated porosity and the same other settings as Case 1. The mismatch results are shown in Figure 29(b). This is Case 2. Finally, increasing the number of perturbation locations and enlarging the range of propagate perturbations may reduce the mismatch levels, the permeability conditional realization #1 was updated by the methodology with co-simulated porosity, perturbation locations shown in Figure 15 plus one location near the well with the highest mismatch after nineteen iterations, and anisotropy ranges of 500m in the Y

direction and 800m in the X direction. The mismatch results are shown in Figure 29(c). This is Case 3. The comparison of the three cases is shown below.

Case	Porosity	Perturbation Locations	Range		Original Mismatch		Updated Mismatch	
			X	Y	Pressure	Rate	Pressure	Rate
1	True	Figure 25	500	500	654.93	54.78	217.15	19.82
2	Co-simulated	Figure 25	500	500	2478.01	712.50	1231.53	310.86
3	Co-simulated	Figure 15	500	800	2478.01	712.50	578.70	261.60

From Figure 29 and the table above, it can be seen that the porosity model has a large effect on mismatch change with iteration and the cases with co-simulated porosity reached a higher mismatch levels than with true porosity. Cosimulated porosity is reasonable in practice.

Comparison of Linear Approximation and Flow Simulation Results

Linearized formulas for pressure and flow rate reservoir behavior are used for optimization in the methodology. The calculated results from the linearized formulas vs. the simulation results at the two iterations in one application to the original permeability realization #1, iteration 5 and iteration 12, are shown in Figures 30 and 31. Only the graphs with visible difference between the linear approximation and the simulation results are shown. Figures 30 and 31 show that the reservoir behaviors obtained by means of the linear approximation and flow simulation are very close in the view of the mismatch calculation, which means that using the linear approximation of reservoir behavior in the optimization of the proposed methodology is suitable.

Conclusions

Application of the proposed method to the synthetic reservoir shows that the resulting reservoir models correspond to the reduced pressure mismatch and rate mismatch. The methodology works for all realizations. The linear approximation is an effective method to obtain well behaviours.
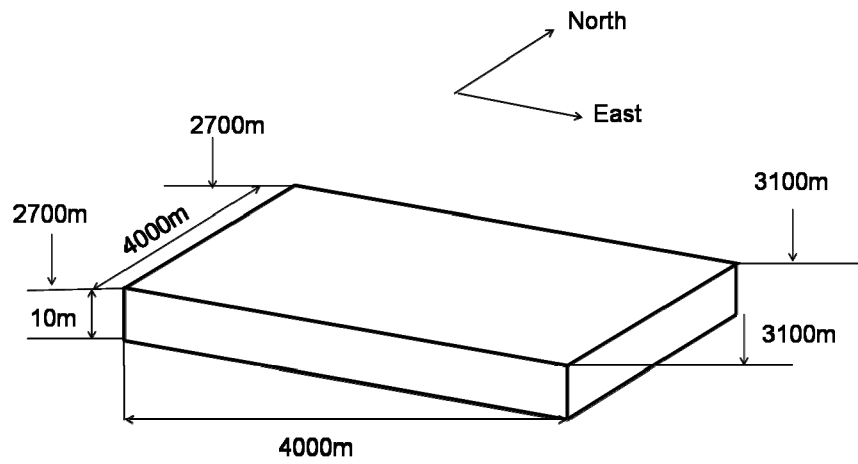
Figure 1: Schematic illustration of the synthetic example.
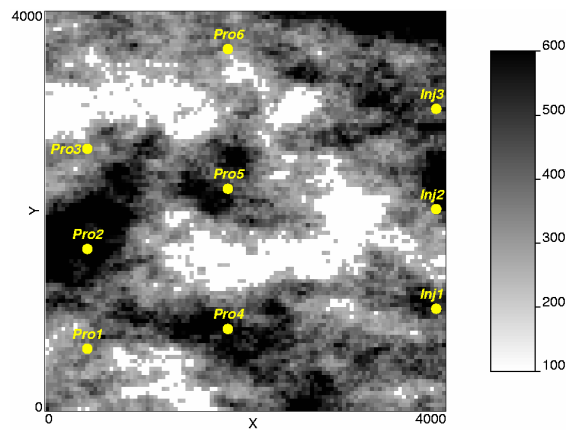
(a) Reference Permeability
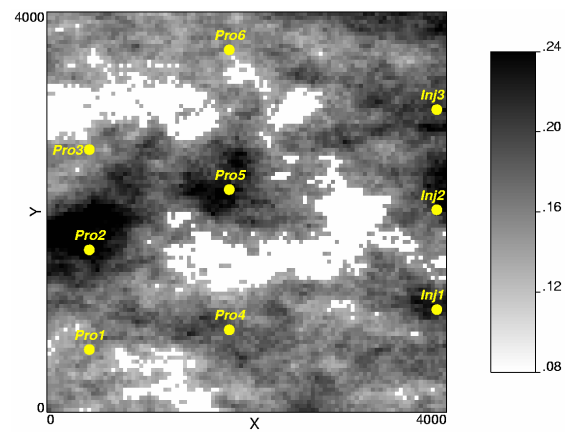
(b) Reference Porosity

Figure 2: Reference permeability (mD) and porosity (fraction) models.
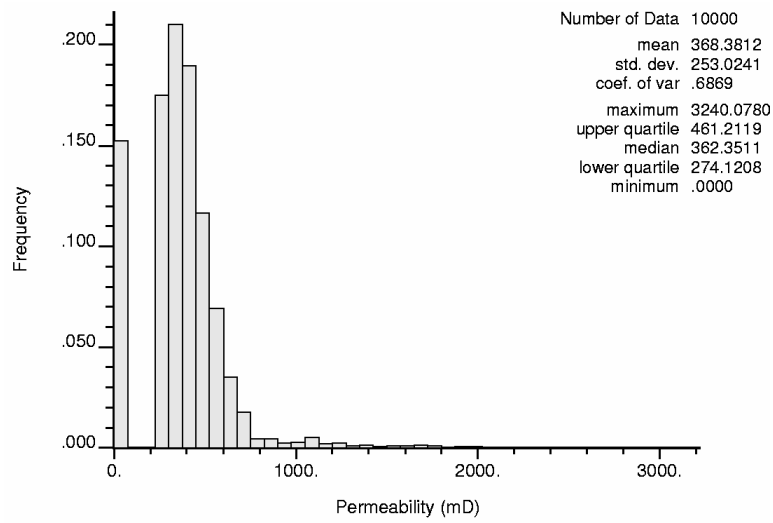
(a) Reference Permeability
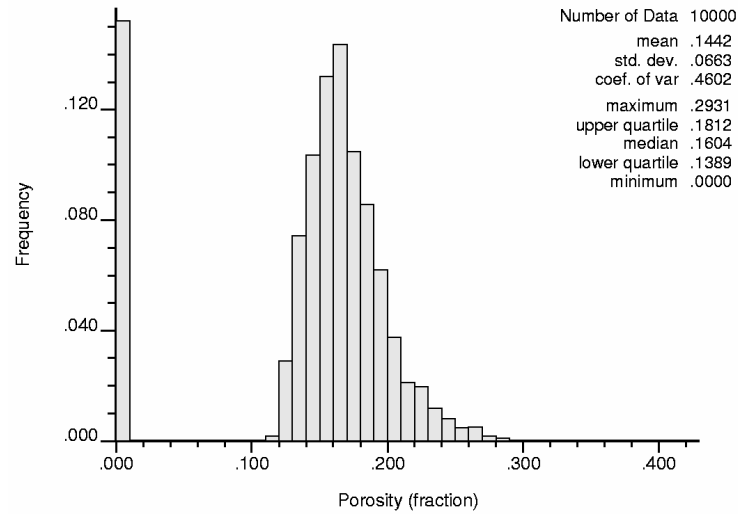
(b) Reference Porosity

**Figure 3:** Histograms of the true permeability and porosity models.
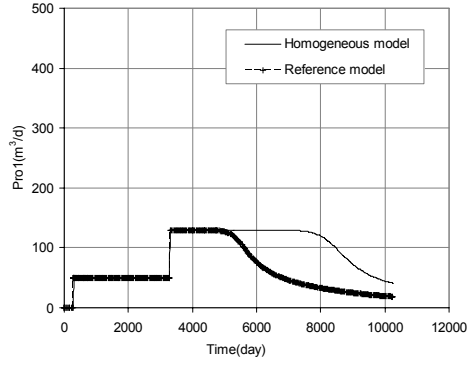
(a) Well Pro1
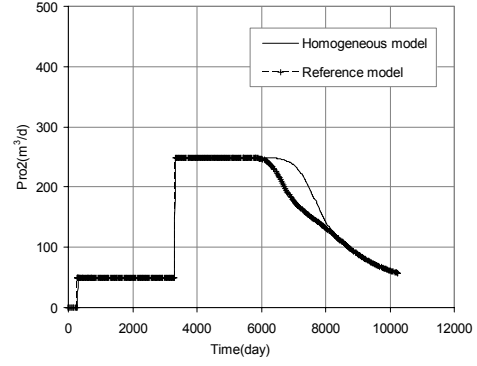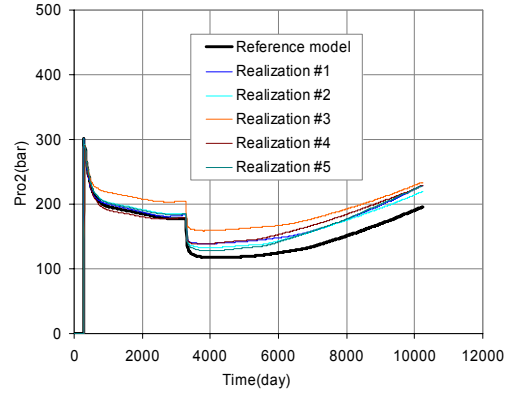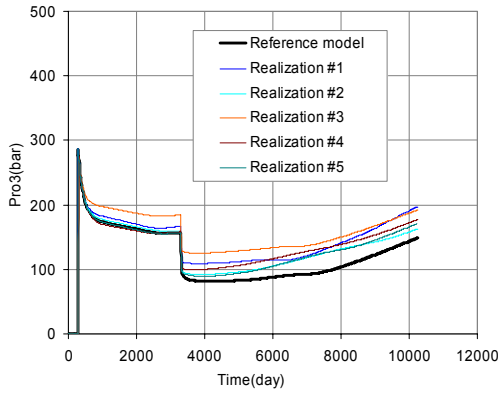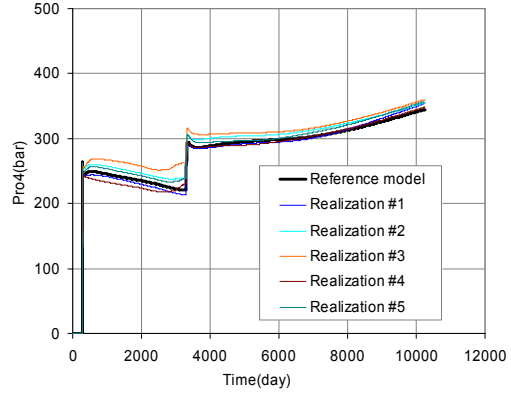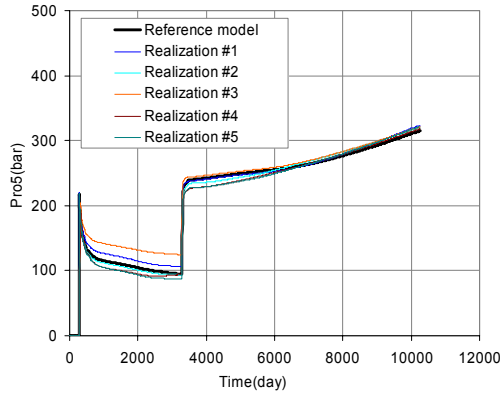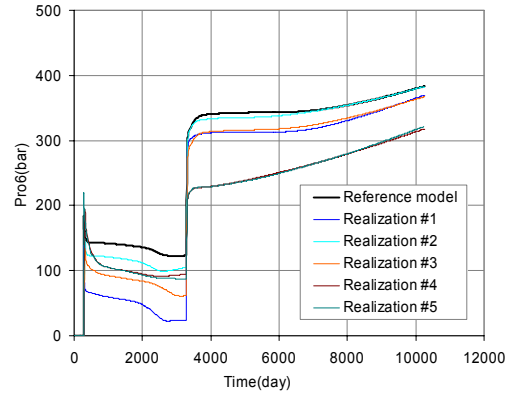
(b) Well Pro2
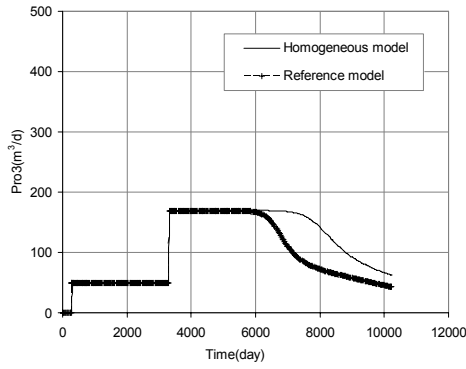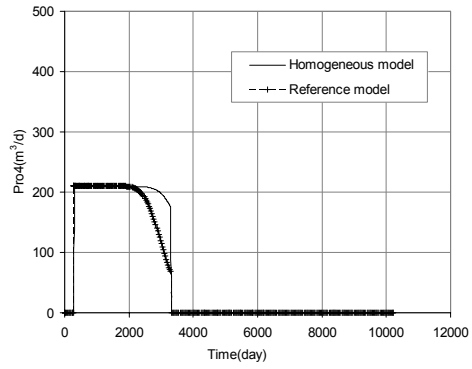
(c) Well Pro3
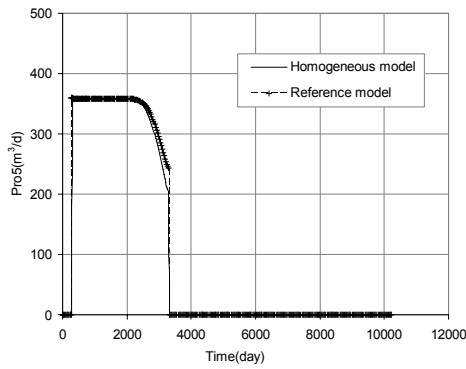
(d) Well Pro4
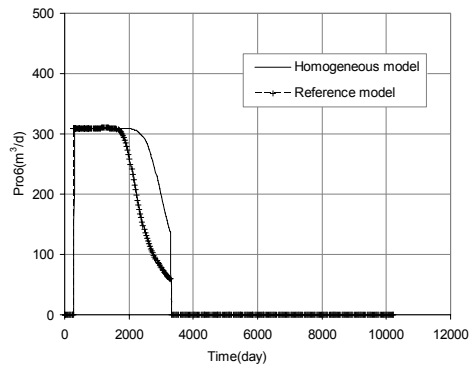
(e) Well Pro5

(b) Well Pro6

Figure 4: Well oil production rates at six producers for the reference model and homogeneous model.
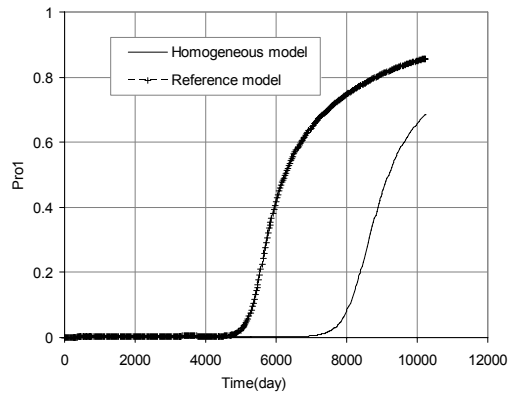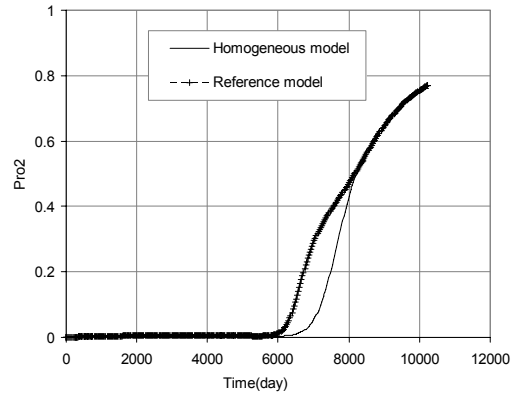
(a) Well Pro1
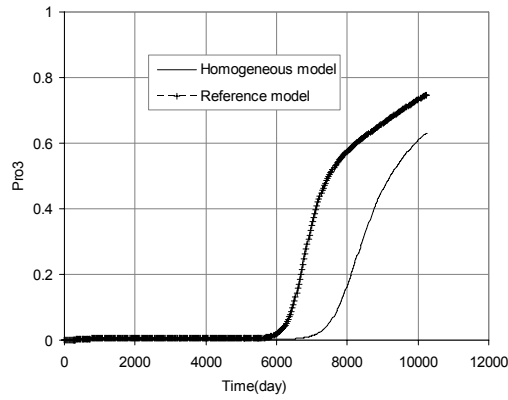
(b) Well Pro2
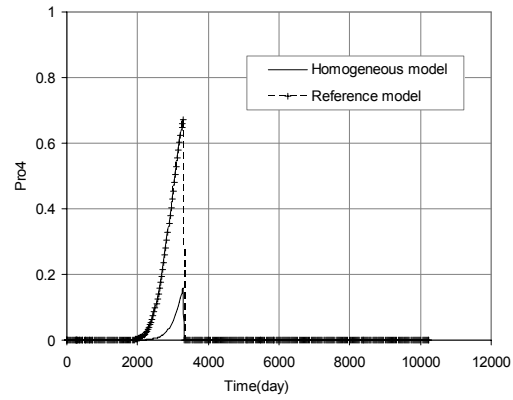
(c) Well Pro3
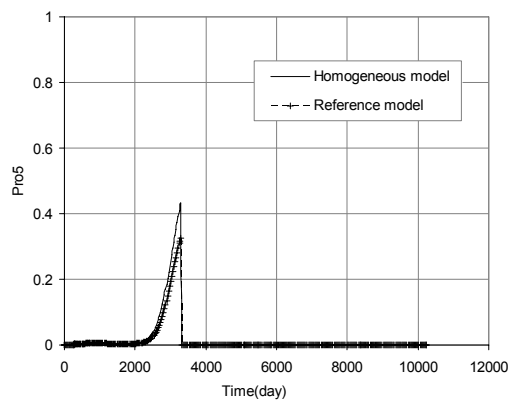
(d) Well Pro4
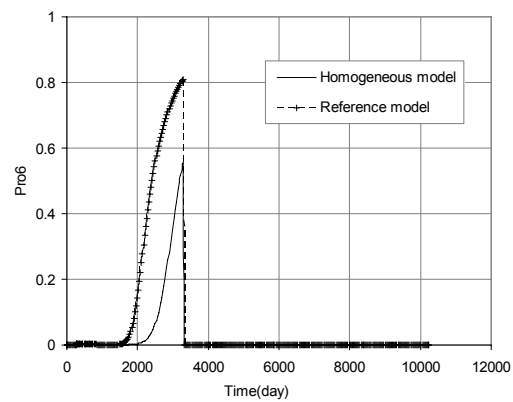
(e) Well Pro5

(f) Well Pro6

Figure 5: Well water cuts at six producers for the reference model and homogeneous model.
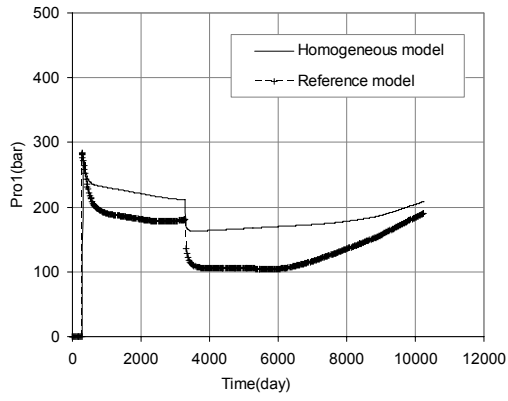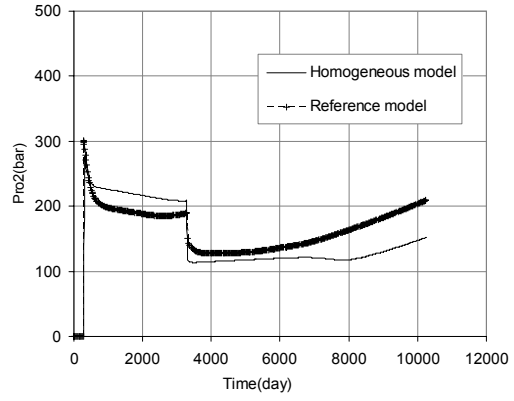
(a) Well Pro1
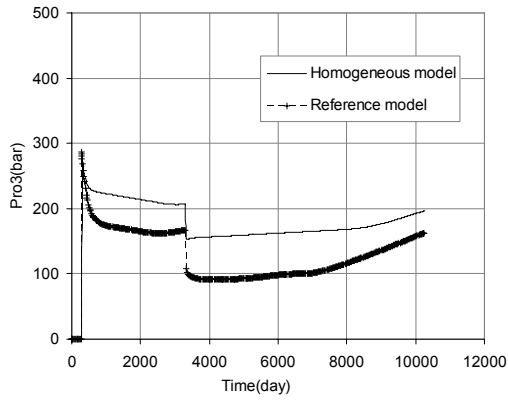
(b) Well Pro2
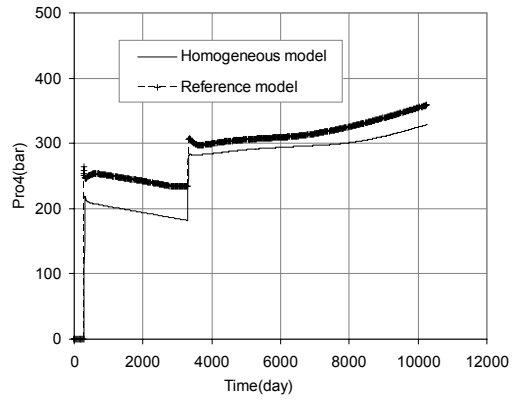
(c) Well Pro3
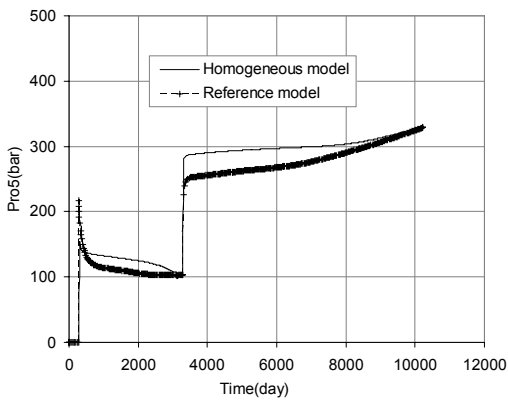
(d) Well Pro4
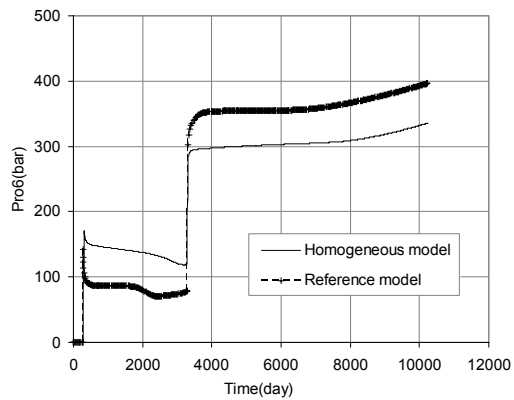
(e) Well Pro5

(f) Well Pro6

Figure 6: Well bottom hole pressure at six producers for the reference model and homogeneous model.

(a) Well Inj1

(b) Well Inj2

(c) Well Inj3
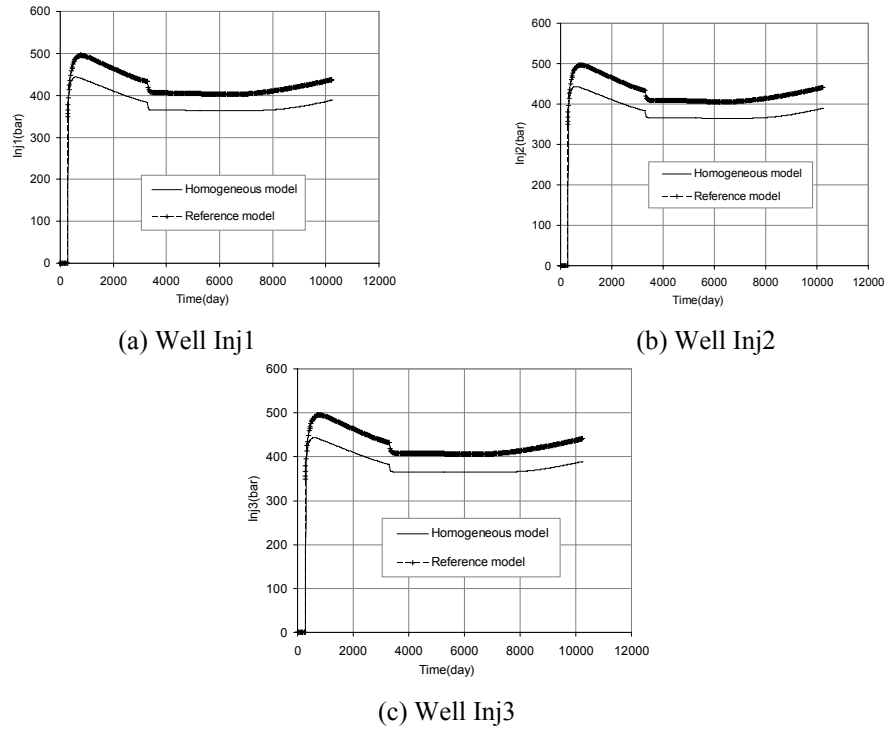
Figure 7: Well bottom hole pressure at three injectors for the reference and homogeneous model.

(a) Field Pressure (FPR)

(b) Field Oil Production Rate (FOPR)

(c) Field Water Production Rate (FWPR)
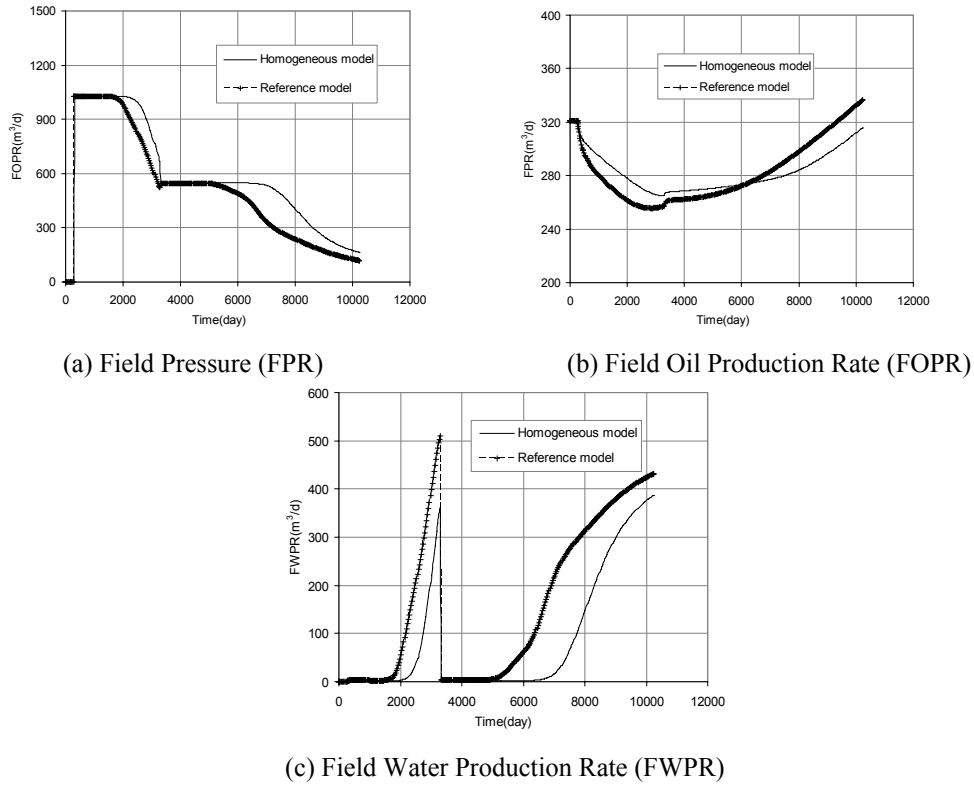
Figure 8: Field behaviours for reference model and the homogeneous model.
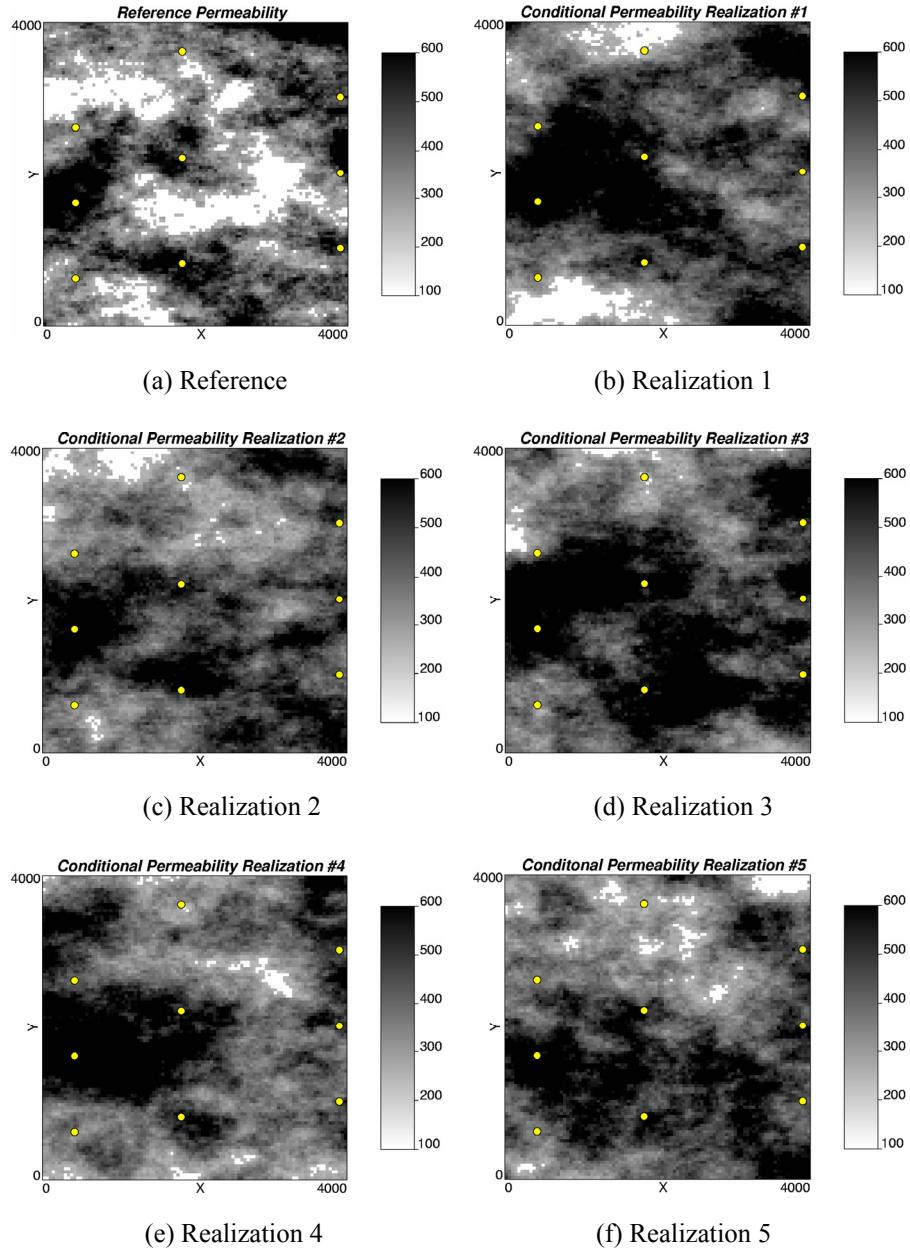
Figure 9: Reference and the five conditional permeability realizations.
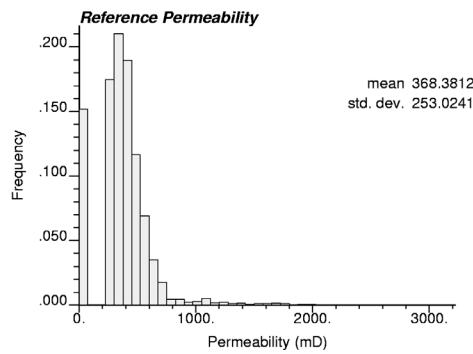
(a) Reference
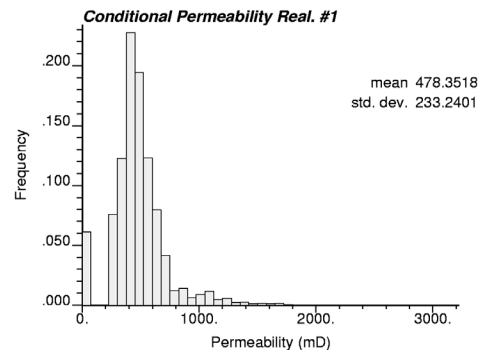
(b) Realization 1
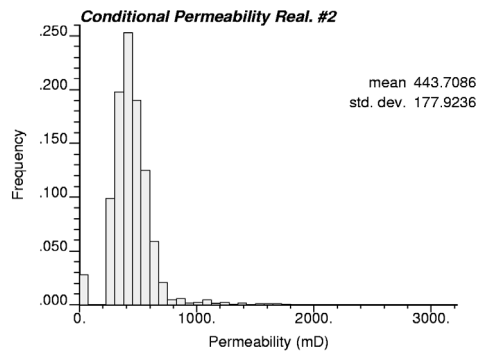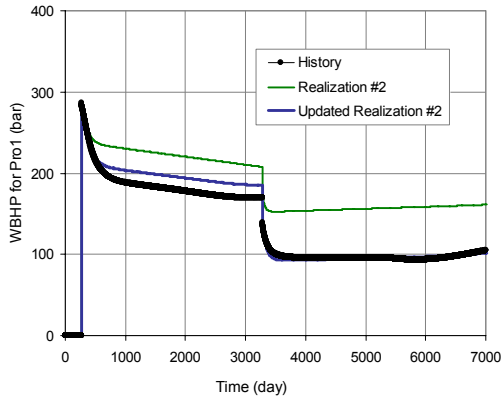
(c) Realization 2
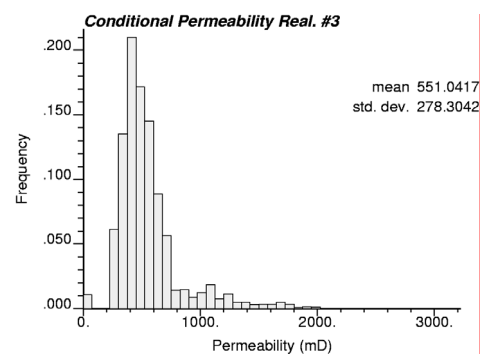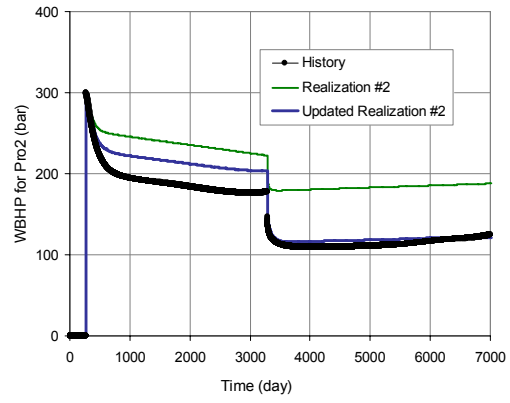
(d) Realization 3
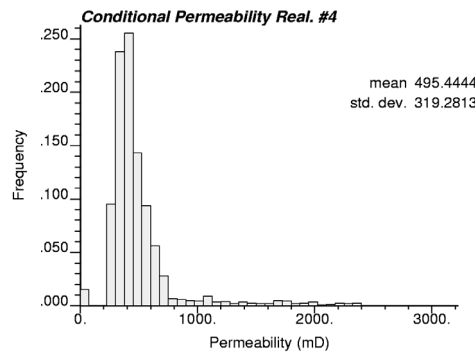
(e) Realization 4
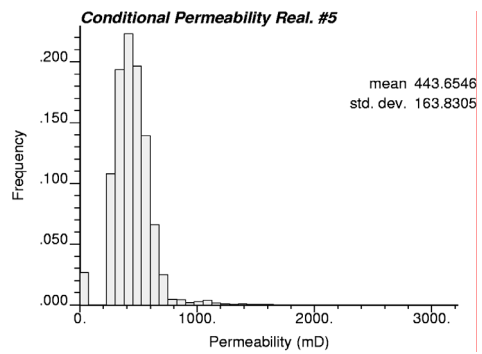
(f) Realization 5

Figure 10: Histograms for the five conditional realizations and reference model.
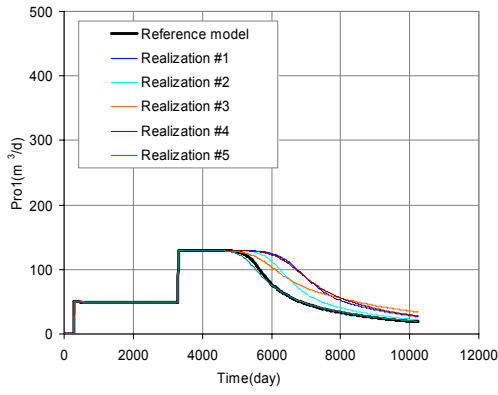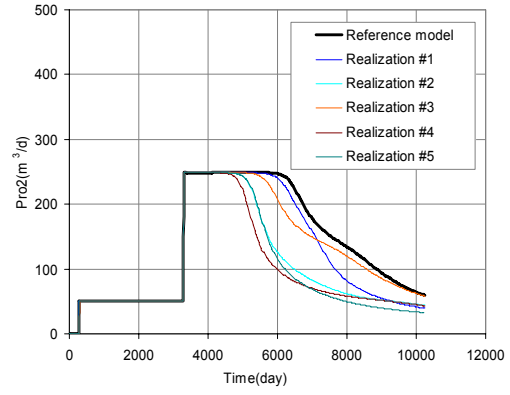
(a) Well Pro1
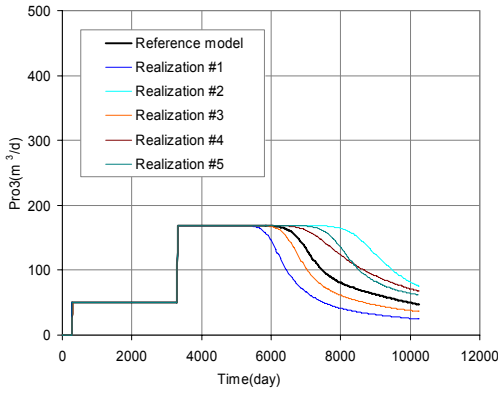
(b) Well Pro2
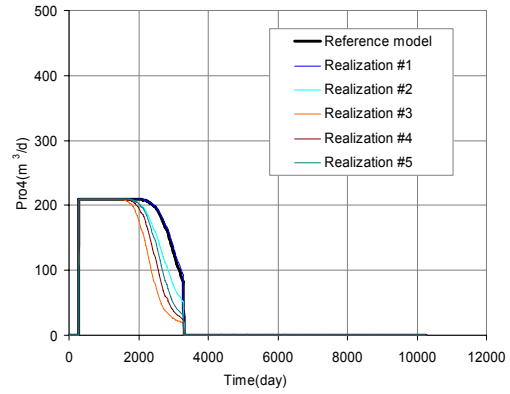
(c) Well Pro3
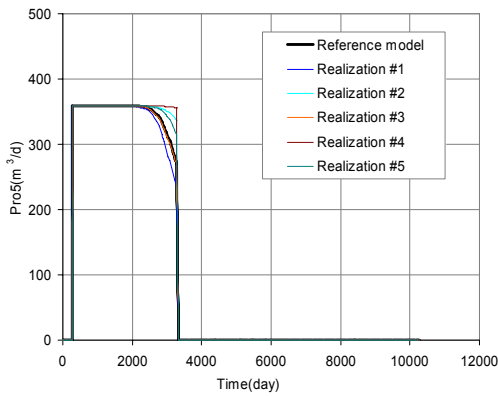
(d) Well Pro4
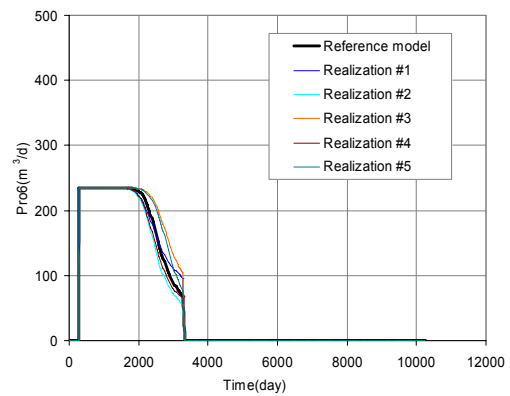
(e) Well Pro5

(b) Well Pro6

Figure 11: Well oil production rates at six producers for the five conditional realizations and the reference model.
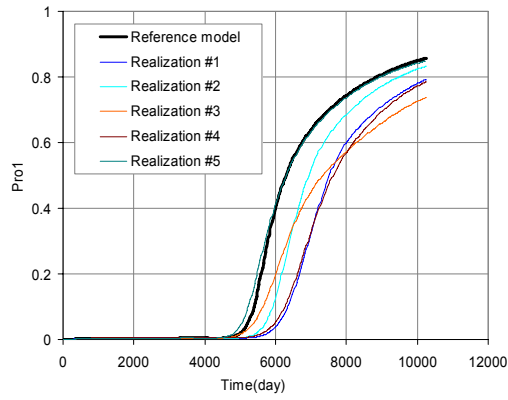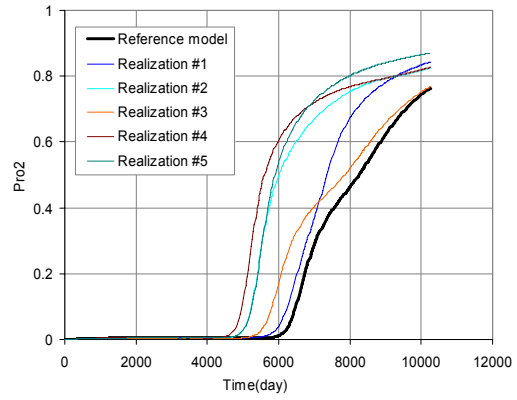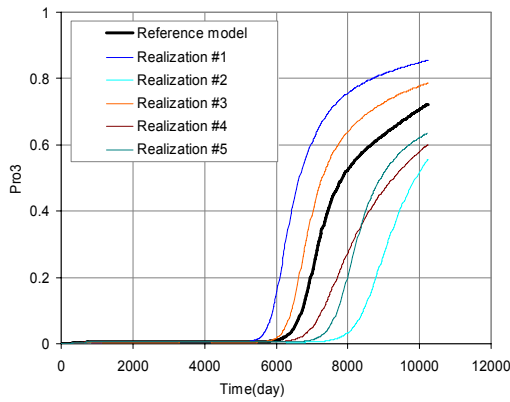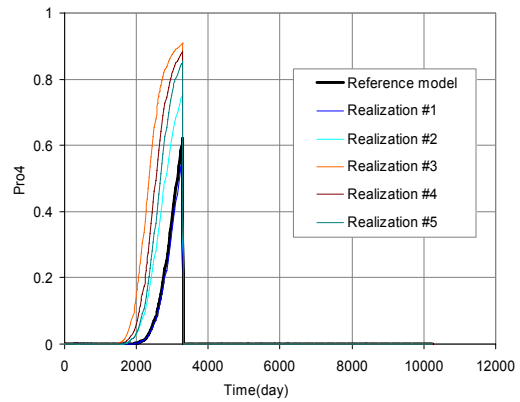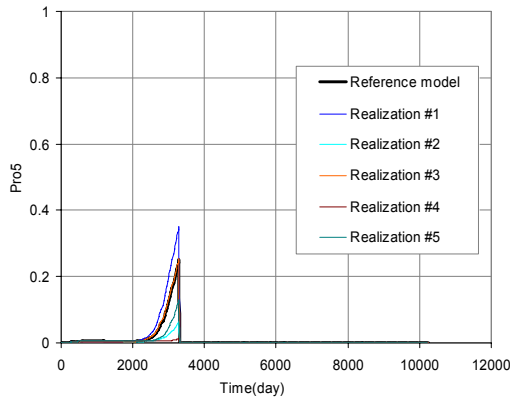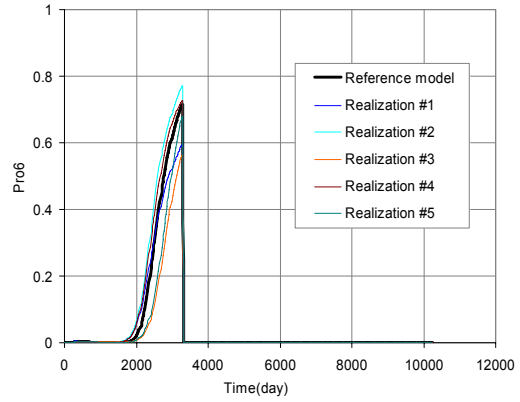
Figure 12: Well water cuts at six producers for the five conditional realizations and the reference model.
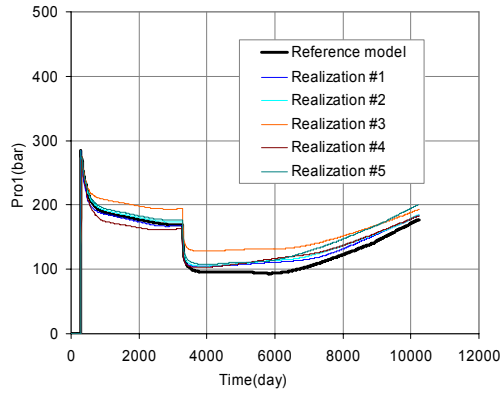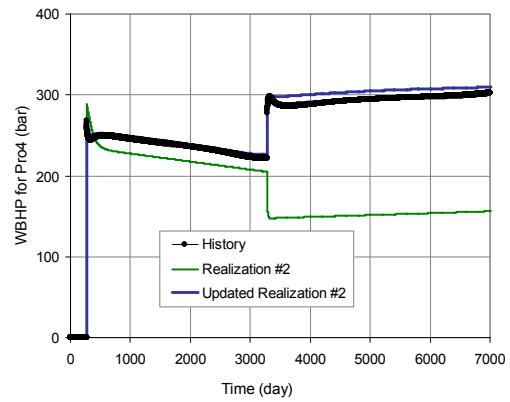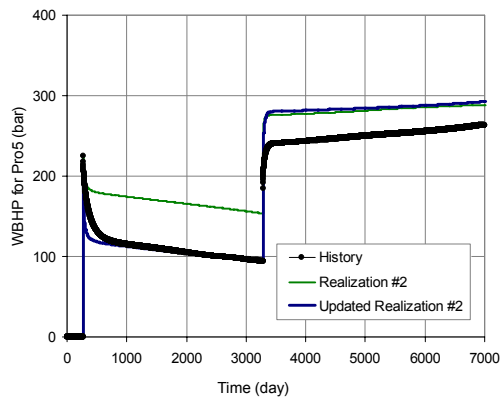
(a) Well Pro1   (b) Well Pro2

(c) Well Pro3   (d) Well Pro4

(e) Well Pro5   (f) Well Pro6

Figure 13: Well bottom hole pressure at six producers for the five conditional realizations and the reference model.

(a) Well Inj1   (b) Well Inj2

(c) Well Inj3
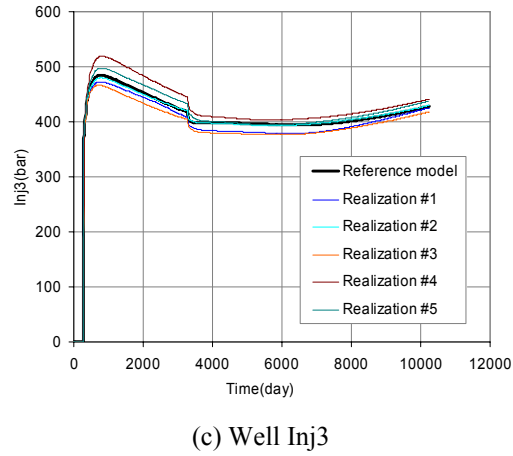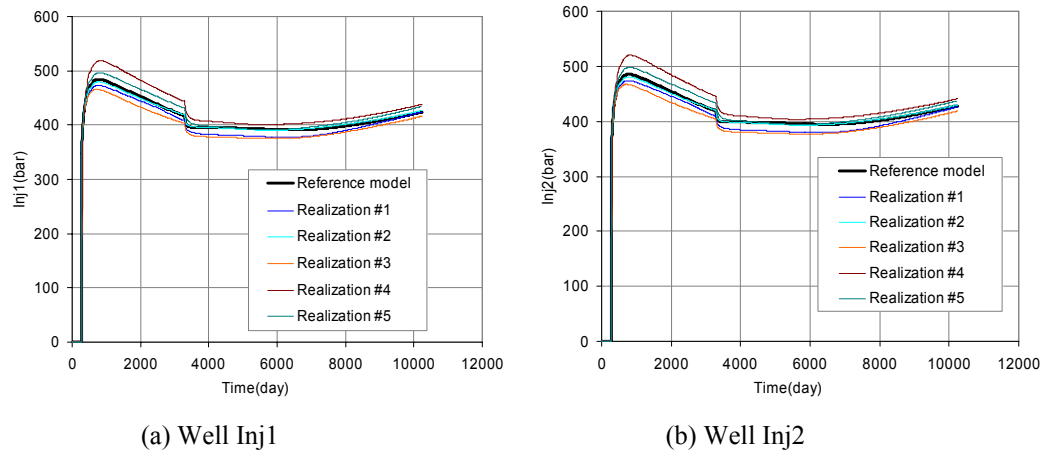
Figure 14: Well bottom hole pressure at three injectors for the five conditional realizations and the reference model.
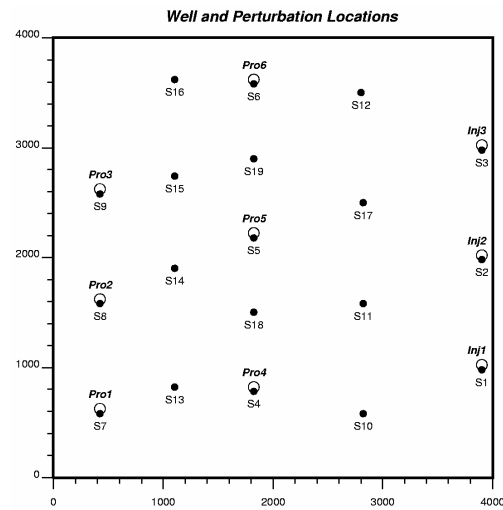
Figure 15: Well locations and perturbation locations.
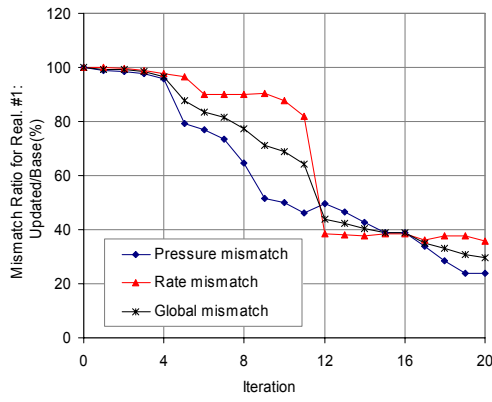
(a) Realization 1
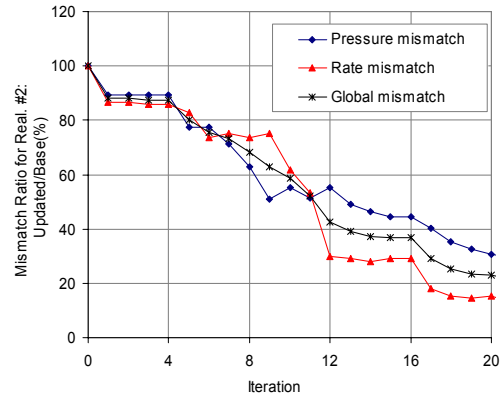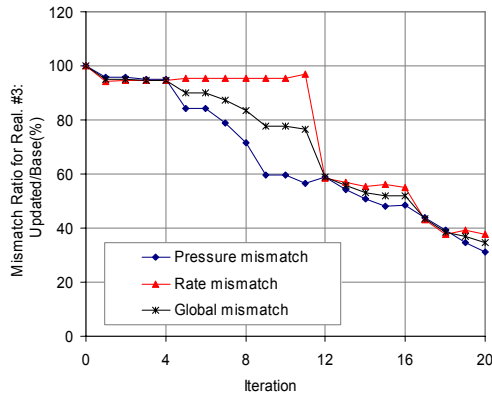
(b) Realization 2
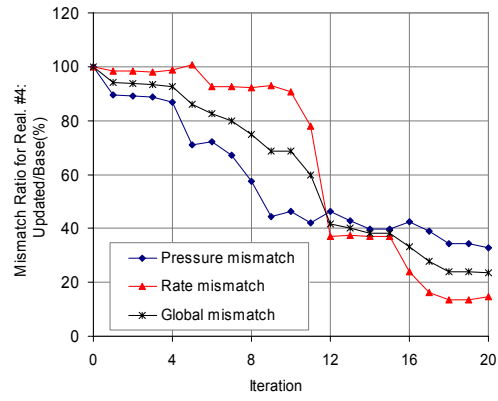
(c) Realization 3

(d) Realization 4
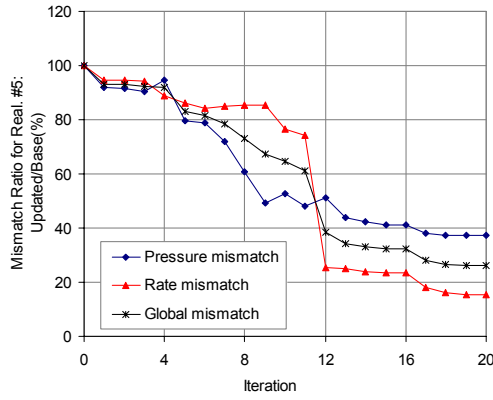
(f) Realization 5

Figure 16: Mismatch ratio for the five realizations.
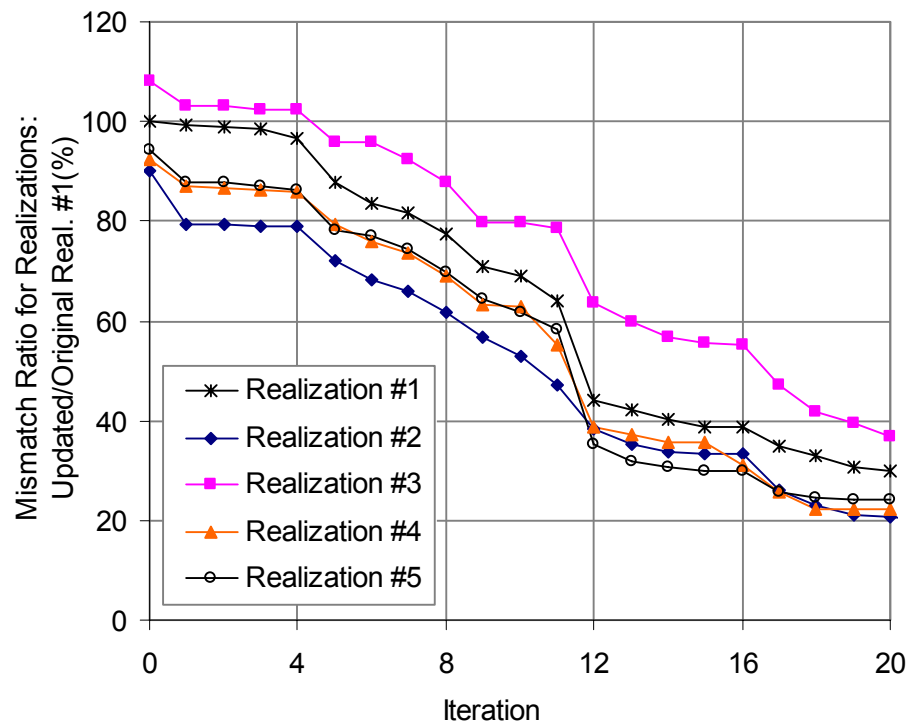
Figure 17: Comparison of the global mismatch versus iteration for the five realizations.
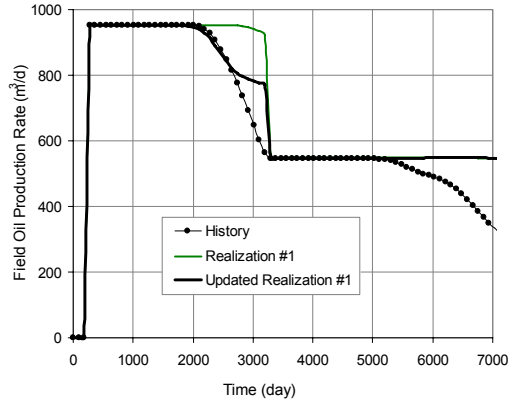
(a) Realization 1
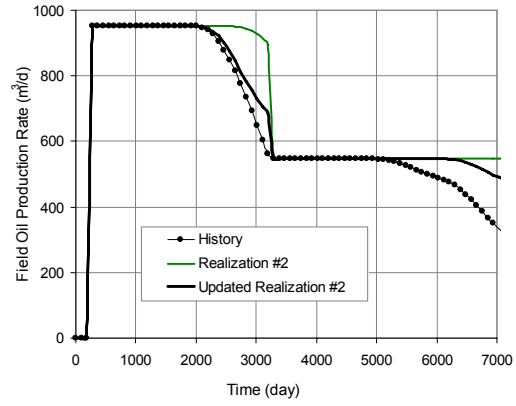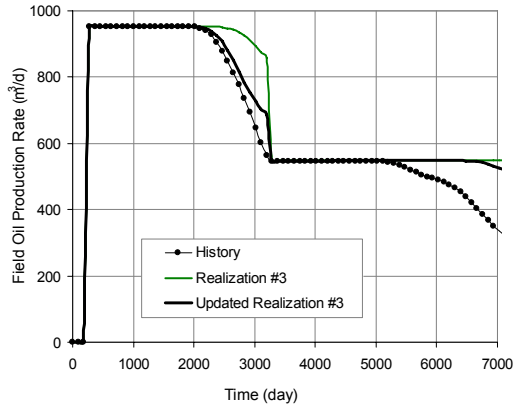
(b) Realization 2
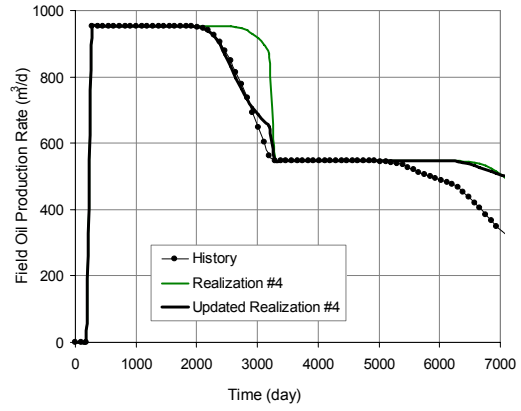
(c) Realization 3

(b) Realization 4
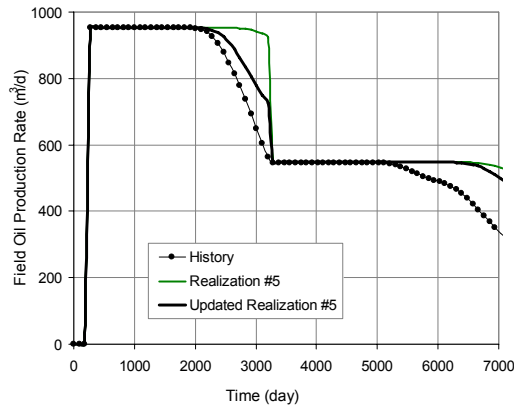
(e) Realization 5

Figure 18: Comparison of the simulation results of field oil production rate for original realizations, updated realizations and historical data.
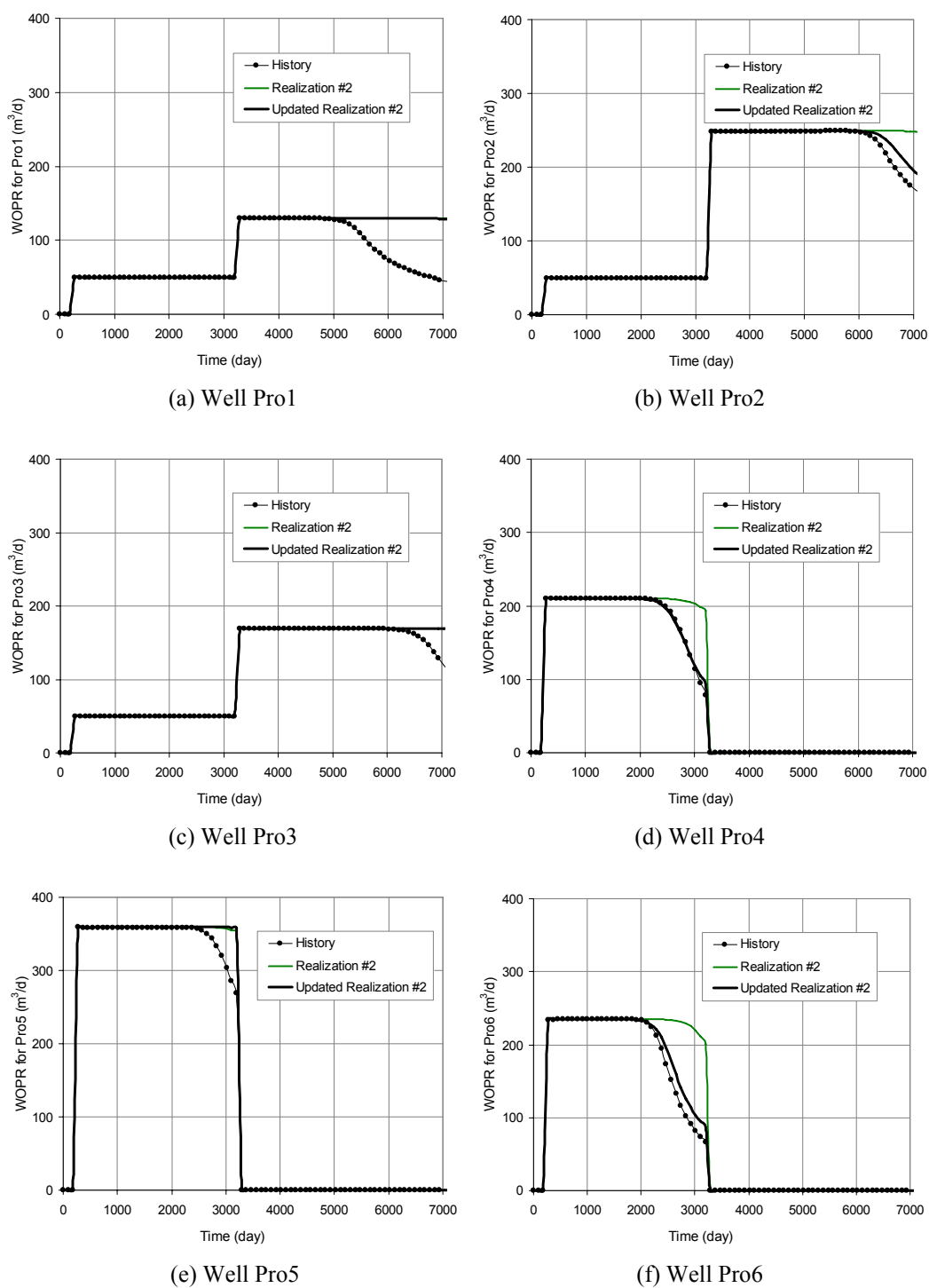
Figure 19: Comparison of the simulation results of well oil production rate for original realizations, updated realizations and historical data.

(a) Well Pro1

(b) Well Pro2
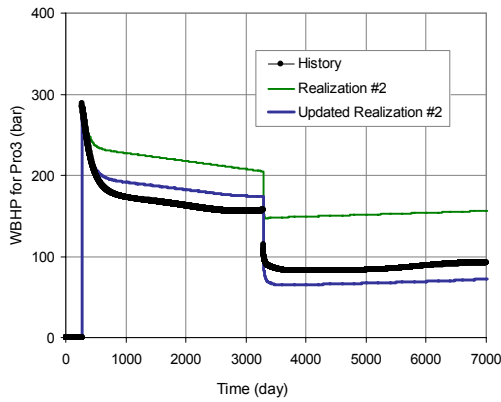
(c) Well Pro3

(d) Well Pro4
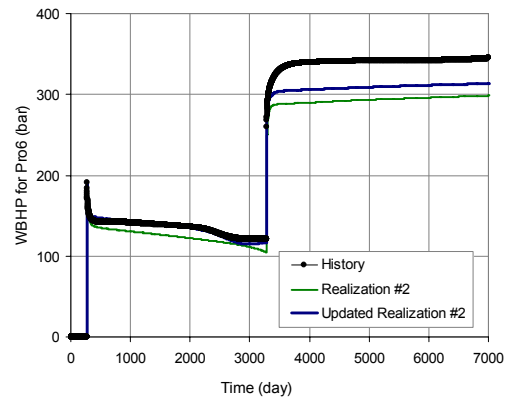
(e) Well Pro5

(f) Well Pro6

Figure 20: Comparison of the simulation results of well bottom-hole pressure at six producers.
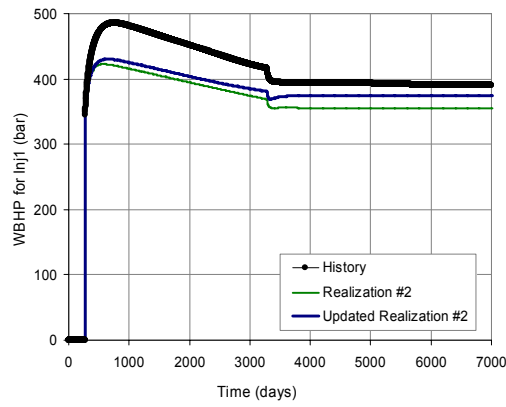
(a) Well Inj1
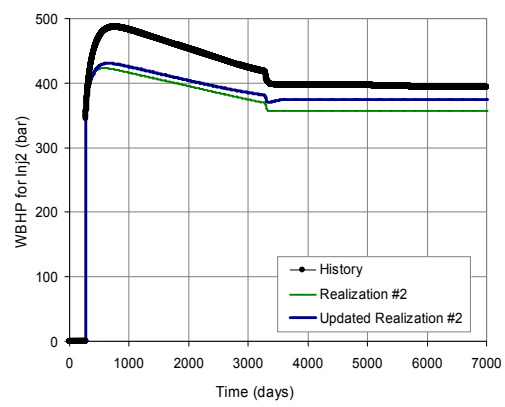
(b) Well Inj2
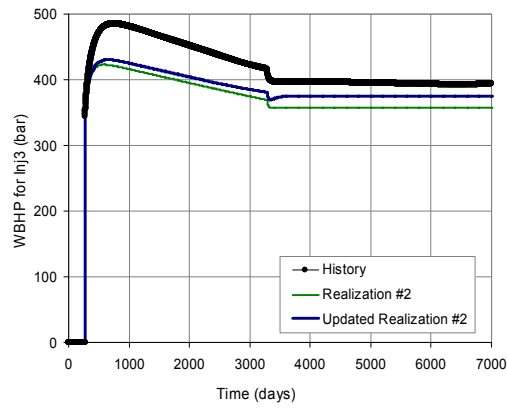
(c) Well Inj3

Figure 21: Comparison of the simulation results of well bottom-hole pressure at three injectors.

(a) Reference

(b) Updated Realization 1

(c) Updated Realization 2

(d) Updated Realization 3

(e) Updated Realization 4

(f) Updated Realization 5
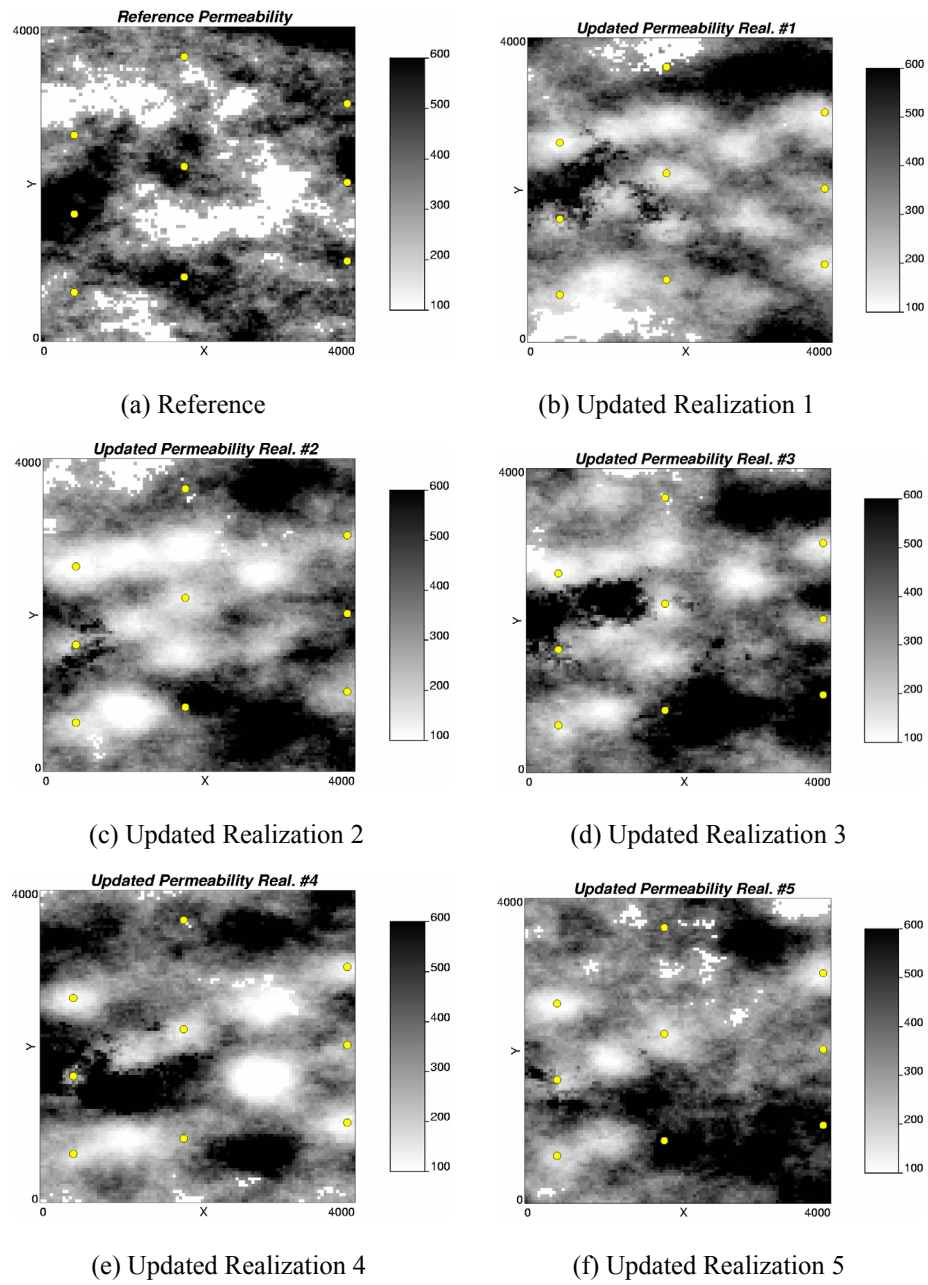
Figure 22: Comparison of the five updated realizations and reference model.
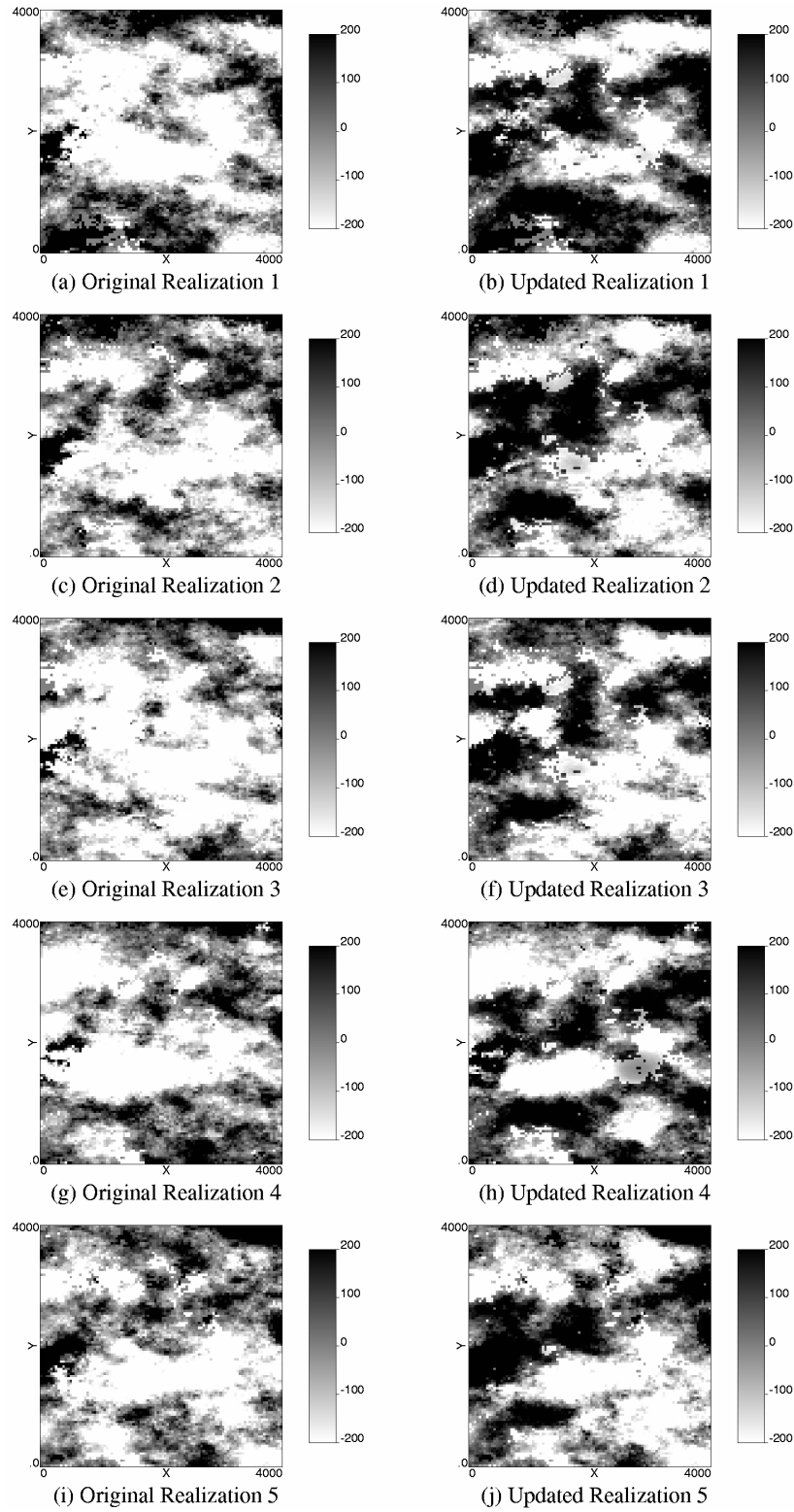
**Figure 23:** Permeability difference between true and the conditional realizations.

(a) Original Realization 1   (b) Updated Realization 1

(c) Original Realization 2   (d) Updated Realization 2

(e) Original Realization 3   (f) Updated Realization 3

(g) Original Realization 4   (h) updated Realization 4

(i) Original Realization 5   (j) Updated Realization 5
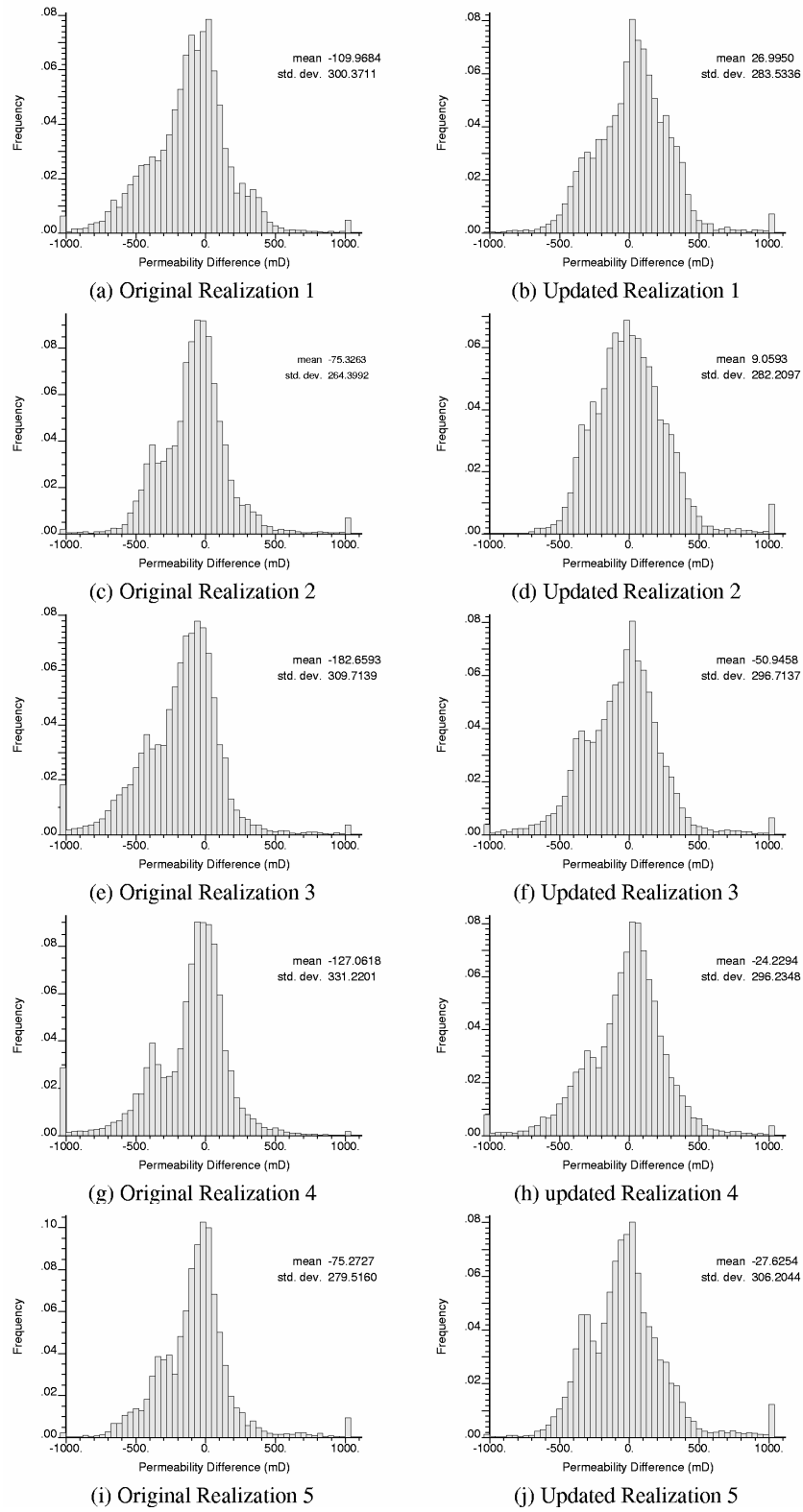
Figure 24: Histograms of permeability difference between true and the conditional realizations.
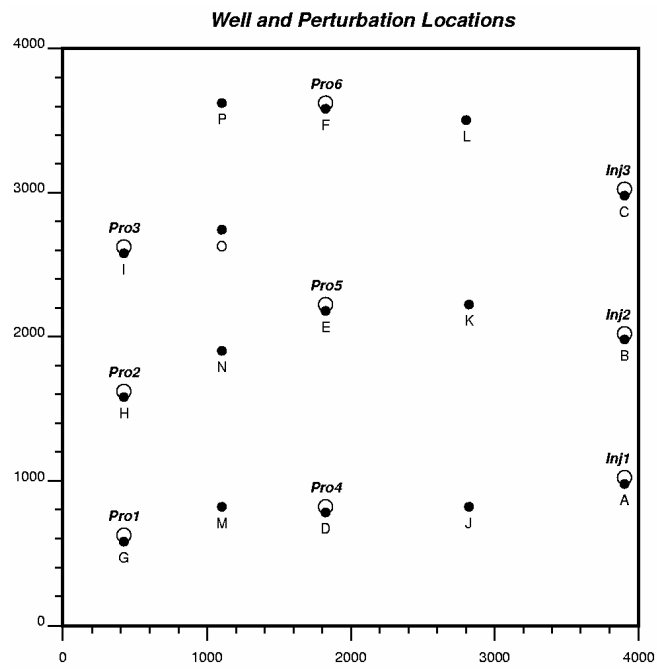
Figure 25: Perturbation locations and well locations.
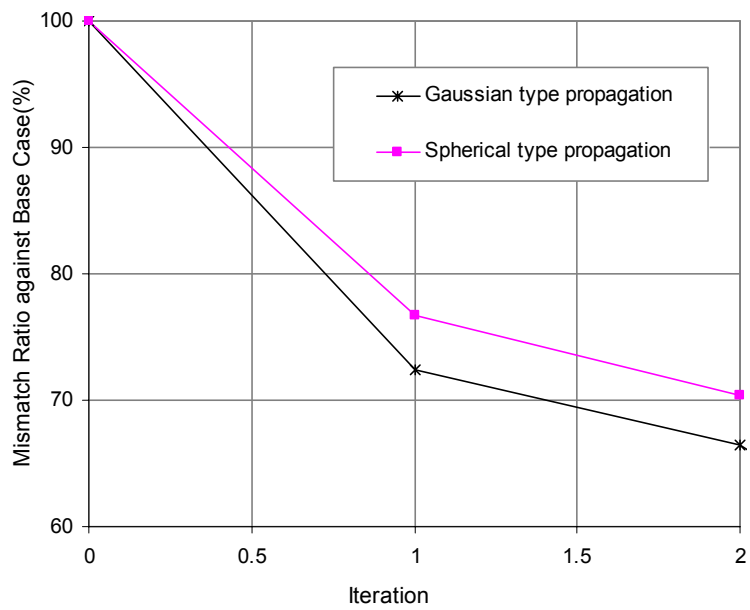
Figure 26: Mismatch change for different propagation types.
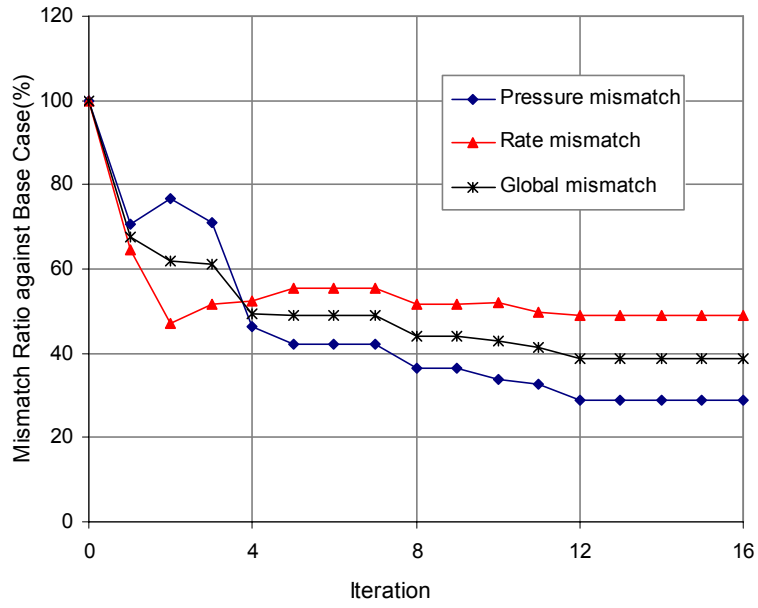
(a) Perturbations far from well locations at first

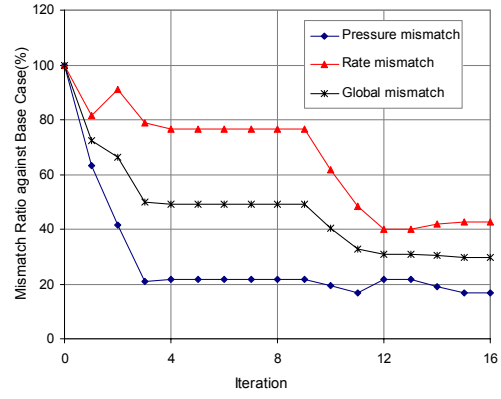(from the first to the last iteration: J, K,L,M,N,O,P,H,F,D,E,G,F,D,H,I)
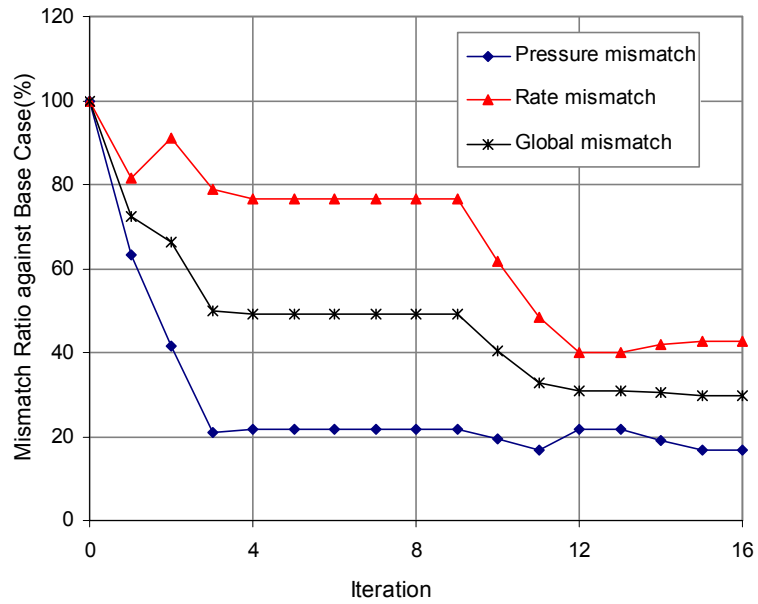
(b) Perturbations near well locations at first
(from the first to the last iteration: H,F,D,E,G,I,H,F,D,J,K,L,M,N,O,P)

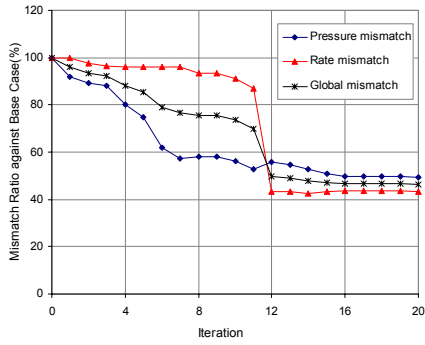**Figure 27:** Mismatch versus iteration in the application with different orders of the selected perturbation locations.
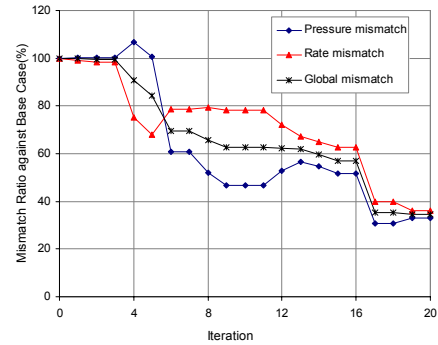
<div align="center">
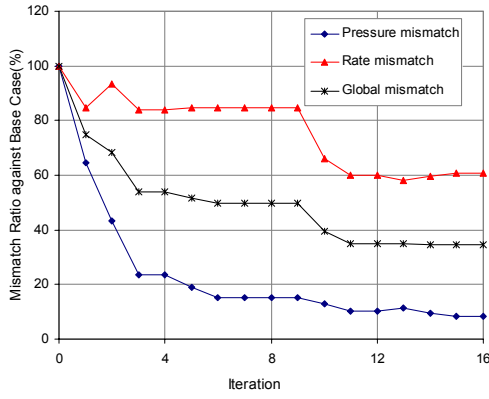
(a) Range of 400m   (b) Range of 500m

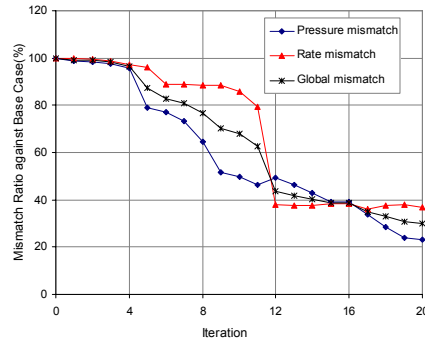</div>

Figure 28: Mismatch versus iteration for different ranges of perturbation propagation.
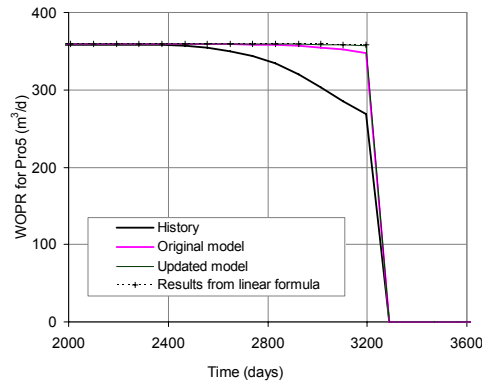

<div align="center">
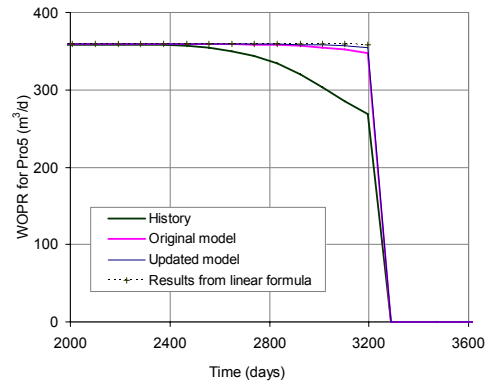
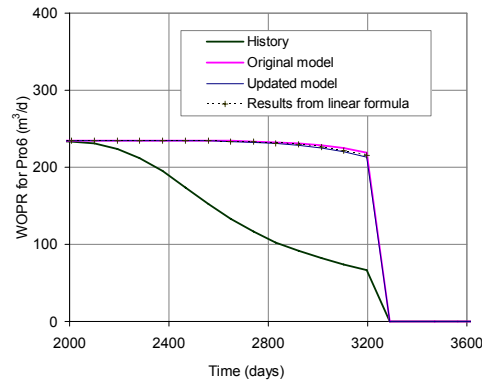(a) Case 1   (b) Case 2

(c) Case 3

</div>

Figure 29: Mismatch change with iterations for the three different cases.
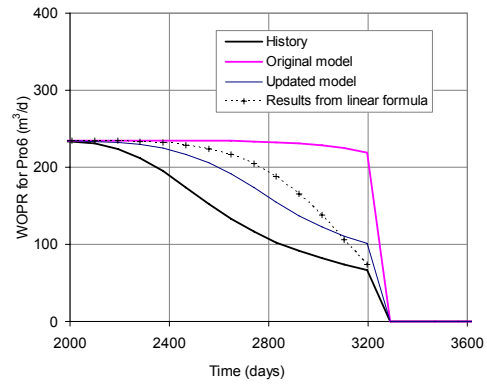
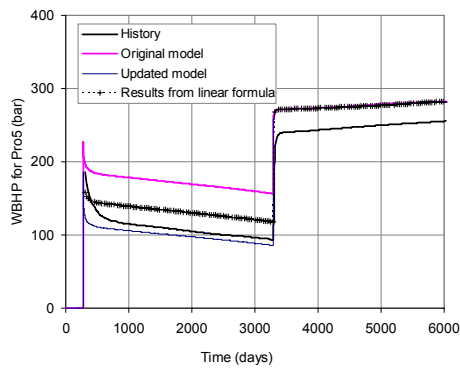(a) Well Pro5, Iteration 5   (b) Well Pro5, Iteration 12
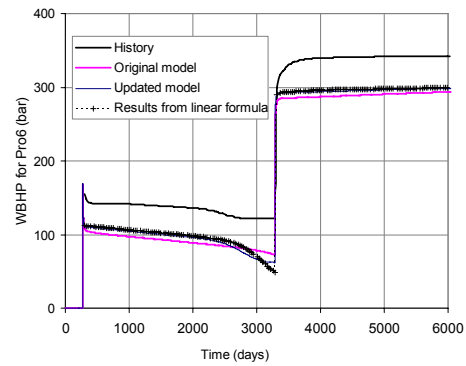
(c) Well Pro6, Iteration 5   (d) Well Pro6, Iteration 12

Figure 30: Comparison of the well production rates from linear approximation and simulation results for the updated model.

(a) Pro5, Iteration 5   (b) Pro6, Iteration 12

Figure 31: Comparison of the well bottom hole pressure from linear approximation and simulation results for the updated model.